Role of the Hydrogen Bond on the Internal Conversion of Photoexcited Adenosine

Ritam Mansour, Josene M Toldo, Mario Barbatti

Role of the Hydrogen Bond on the Internal Conversion of Photoexcited Adenosine

Ritam Mansour,[a] Josene M. Toldo,[a*] and Mario Barbatti [a,b*]

[a] *Aix Marseille University, CNRS, ICR, Marseille, France.*
[b] *Institut Universitaire de France, 75231 Paris, France.*

This is the accepted version of the paper published at https://doi.org/10.1021/acs.jpclett.2c01554

ABSTRACT. Experiments and theory have revealed that hydrogen bonds modify the excited-state lifetimes of nucleosides compared to nucleobases. Nevertheless, how these bonds impact the internal conversion is still unsettled. This work simulates the nonadiabatic dynamics of adenosine conformers in the gas phase with and without hydrogen bonds between the sugar and adenine moieties. The isomer containing the hydrogen bond (*syn)* exhibits a significantly shorter excited-state lifetime than the one without it (*anti*). However, internal conversion through electron-driven proton transfer between sugar and adenine plays only a minor (although non-negligible) role in the photophysics of adenosine. Either with or without hydrogen bonds, photodeactivation preferentially occurs following the ring puckering pathways. The role of the hydrogen bond is to avoid the sugar rotation relative to adenine, shortening the distance to the ring puckering internal conversion.

DNA nucleobases and nucleosides are basic structural units of the building blocks of life, the nucleic acids. They strongly absorb in the ultraviolet (UV) region (240–290 nm), which could potentially cause substantial photochemical damage.[1, 2] However, DNA is remarkably photostable thanks to several efficient deactivation processes occurring on time scales ranging from subpicosecond in isolated nucleosides and base pairs to a few hundreds of picoseconds in DNA strands.[1, 3-8] In isolated nucleobases, these processes are due to ultrafast internal conversion to the ground state, triggered mainly by conical intersections involving puckering of the heterocyclic ring.[9-15] In nucleosides, the presence of the sugar ring can open up an additional internal conversion pathway induced by the hydrogen bond between the nucleobase and a pentose's hydroxyl.[16-18]

Indeed, the shorter lifetime observed for some nucleosides compared to their nucleobases has been attributed to an efficient internal conversion induced by the presence of the sugar ring.[19-21] Tuna *et al.* investigated the photodeactivation of adenosine using the algebraic diagrammatic construction to the second-order [ADC(2)] computational method.[16] They considered two conformers, *syn* and *anti*, exhibiting an intramolecular hydrogen bond between the sugar and the adenine moiety. Exploring the excited-state reaction pathways, they claimed that this hydrogen bond should favor the internal conversion through electron-driven proton transfer (EDPT) for both conformers. The EDPT mechanism, which corresponds to a hydrogen transfer mediated by a charge-transfer state, creates a conical intersection with the ground state. Still according to Tuna *et al.*, it would be responsible for shortening adenosine's excited-state lifetime.

Subsequently, De Camillis *et al.*[19] invoked EDPT to rationalize their experimental results from pump-probe ionization of nucleosides in the gas phase. They suggested that this mechanism could also be operative in other nucleosides since the lifetimes for internal conversion to the ground state in adenosine, cytidine, and thymidine are reduced by a factor of two compared to their respective nucleobases. An exception was guanosine which displayed longer lifetimes.

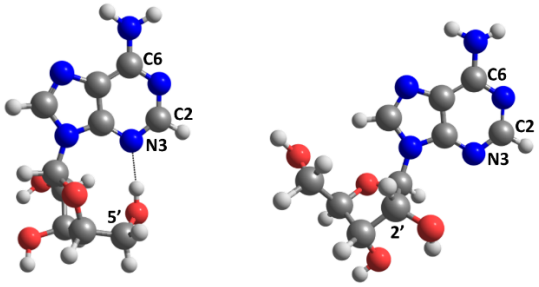

Figure 1. *Syn* and *anti* conformers of adenosine optimized at ADC(2)/SV(P).

Zhao *et al.* investigated the possibility of EDPT being also valid for guanosine, the other canonical purine nucleoside.[17] (In their paper, they refer to EDPT as excited-state intramolecular proton transfer.) Exploring the internal conversion pathways using time-dependent density functional theory (TDDFT), they showed that the guanosine's deactivation could occur either mediated by a C2-puckered or EDPT intersection. However, their conclusions differed from those reported by Tuna *et al.*[16] For guanosine, although both pathways were energetically accessible, the C2-puckering was barrierless, while the EDPT would need activation energy of 0.7 eV from the S_1 minimum. They concluded that both pathways could coexist, but the probability of internal conversion occurring through the ring puckering would be higher.

The importance of EDPT has also been questioned for solvated nucleosides. For pyrimidine nucleosides in water, energy barriers of ~0.6 eV were reported for the intramolecular hydrogen transfer.[22, 23] These high activation energies would prevent the hydrogen from being transferred in the sub-ps time scale. Moreover, a recent experimental-theoretical paper reported that the primary deactivation mechanism for uridine in water is the ring puckering induced by the hydrogen out-of-plane bending on the hydroxyl group of the sugar.[3]

At this point, the relevance of EDPT for the nucleosides' internal conversion remains undefined. We decided to take a step back and assess the role of the hydrogen bond in the most fundamental prototypical case, adenosine in the gas phase. We simulated the excited-state nonadiabatic dynamics of conformers with and without a hydrogen bond (Figure 1) using surface hopping to appraise the preponderance of the EDPT and ring puckering mechanisms explicitly.

Adenosine in the gas phase has multiple conformers.[24] We worked on two of them, a *syn* conformer with a hydrogen bond and an *anti* conformer without it. We do not expect these two conformers to be particularly relevant for DNA. At the ground state, the *syn* conformer is more stable than the *anti* by 14.2 kcal/mol, while in the excited state, this difference decreases to 12.3 kcal/mol. The vertical excitation energies and state characterization are reported in the Supporting Information SI-1. *Anti* conformers can also form a hydrogen bond using the 2′-OH group.[24] (Tuna *et al.*[16] investigated one of those.) However, we choose to work with a conformation without this hydrogen bond to have baseline results.

We have run four sets of trajectories (see Computational Methods). The first two to compare the conformers, the third to evaluate the impact of the initial excitation energy, and the fourth to assess the influence of the basis set on the results. We start the discussion with the first two sets. In both, the conformers were excited into the lower region of the first absorption band, similarly to the experimental window.[19] We labeled this excitation window LB (low band) to distinguish it from excitations into the band center (CB), discussed later. After the nonadiabatic propagation, the excited-state lifetime is obtained by fitting the state occupation with the exponential decay function

$$f(t) = y_0 + (1 - y_0)\, e^{-(t-\tau_1)/\tau_2}, \qquad (1)$$

where τ_1 is the latency time to initiate the internal conversion, τ_2 is the exponential decay time constant, and y_0 is the fraction of the population remaining in the excited state. The lifetime (τ) is given by $\tau = \tau_1 + \tau_2$. Details about these fittings are reported in SI-2.

The excited-state lifetimes are presented in Table 1. The *anti* conformer's lifetime, 3.5 ps (Set 1), is significantly longer than the *syn* conformer's lifetime, 2.1 ps. At first glimpse, we were tempted to attribute this difference to the EDPT enabled by the hydrogen bond present only in the *syn* conformer. However, only 21% of the *syn* trajectories decay through this pathway. C2- and C6-puckering (their structures are shown in Figure 2 for *syn* and SI-3 Figure S12 for *anti*) are the dominant pathways in both conformers. For the *syn*, puckering is responsible for 79% of the decay, splitting approximately half between C6 and C2 atoms. The hydrogen bond is always present during the *syn* dynamics.

Table 1. Lifetime (τ) and main pathway yields predicted by surface hopping dynamics for *syn*- and *anti*-adenosine computed at ADC(2) with SV(P) (sets 1 to 3) and cc-pVDZ+ (set 4). LB: excitation in the lower region of the first absorption band. CB: excitation at the center of the absorption band. Margins of errors for a 95% confidence interval. In all cases, $y_0 = 0$ [Eq. (1)].

Set	τ (ps)	% C2 puckering	% C6 puckering	Total puckering	% EDPT
1. *anti* (LB)	3.5 ± 0.9	68 ± 13	23 ± 12	91 ± 6	9 ± 8
2. *syn* (LB)	2.1 ± 0.5	41 ± 14	38 ± 13	79 ±11	21 ± 11
3. *syn* (CB)	1.9 ± 0.7	59 ± 18	14 ± 12	73 ± 16	23 ± 15
4. *syn* (CB, cc-pVDZ+)	1.5 ± 0.5	60 ± 18	16 ± 13	76 ±15	20 ± 14

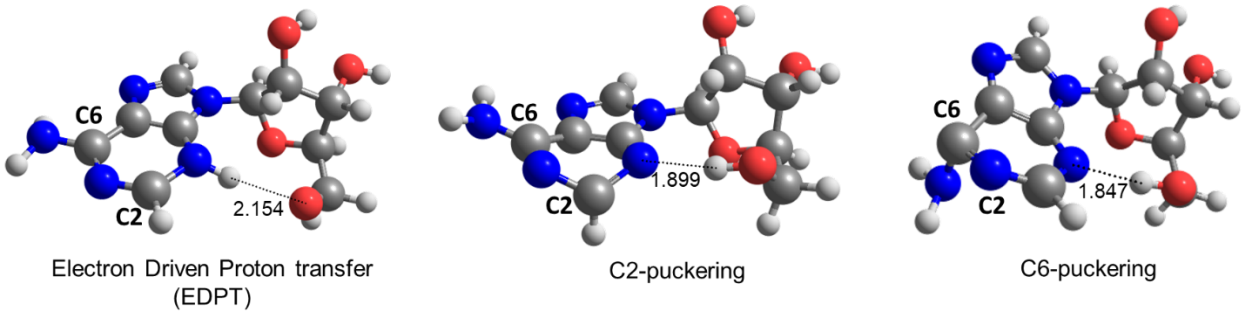

Figure 2. Structures at the S_1/S_0 state crossing for the *syn* conformer.

Interestingly, the *syn* trajectories that followed the EDPT pathway finished at shorter times than those that followed the puckering paths (SI-2 Table S4). As the starting structure of the *anti* conformer does not have the hydrogen bond, the vast majority (90%) of the S_1/S_0 crossings are due to puckering of the adenine ring, mainly at C2 atom (68%). Nevertheless, in a few trajectories, a rotation of the 2'-OH group allowed a hydrogen bond to the N3 atom, enabling EDPT in 9% of the trajectories. In this case, EDPT takes longer than puckering due to the time needed to form the hydrogen bond.

We also investigated the influence of the excitation window by using initial conditions generated from excitations of the *syn* conformer at the center of the absorption band (Set 3). The results are shown in Table 1. The lifetime computed for the two spectral windows, LB and CB, using SV(P) is essentially the same (~2 ps). Puckering is still the dominant, mainly at the C2 atom.

Because of the hydrogen bond between the N3 and the hydrogen on the 5'OH, the dynamics may be sensitive to the basis set, requiring diffuse basis functions. To examine this effect, we ran an additional set of trajectories (Set 4), adding diffuse functions (aug-cc-pVDZ) to N3 and keeping all other atoms with the cc-pVDZ basis set (we refer to it as cc-pVDZ+) to make the dynamics cost affordable. These trajectories were also initially excited into the band center (CB). The cc-pVDZ+ basis set shortens the lifetime to 1.5 ps but does not change the balance between EDPT and puckered intersections. The percentage of trajectories following the hydrogen transfer coordinate was still around 20%. Most of them decay through a C2-puckered intersection.

The dominance of the ring puckering over EDPT raises a few main questions: (i) experiments[19] tell that adenosine's excited state lifetime is shorter than that of adenine, but why would it be so if both follow similar puckering pathways? (ii) Why is the puckering favored over EDPT? (iii) As the EDPT trajectories are, on average, faster than the puckering ones, why is EDPT not the preferential decay pathway? (iv) Why does the hydrogen bond speed up the ring puckering of adenosine in the gas phase?

Based on time-resolved pump-probe spectroscopy, De Camillis *et al.*[19] reported that the excited-state lifetime of adenosine in the gas phase (0.57 ps) is shorter than that of

adenine (1.1 ps, according to Ref. 25). However, if ring puckering dominates the internal conversion like in adenine, we are left with no reason for such time shortening. In fact, our simulations predict the excited-state lifetime of the *syn* conformer (1.5 ps with ADC(2)/cc-pVDZ+) to be comparable to that of adenine (1.4 ps, according to ADC(2)/aug-cc-pVDZ simulations of Ref.[11]). This divergence seems to originate in the experimental setup, not considering the strong ionization potential (IP) variations along the excited-state pathway. In the SI-4, we show that while total pump plus probe energy is enough to ionize adenosine at the ground state minimum geometry, it cannot ionize the molecule along the entire puckering pathways, not even at the S_1 minimum. Thus, adenosine should leave the probe detection window[26] much before the internal conversion, underestimating the excited-state lifetime.

To address the other questions, we calculated the potential energy profiles connecting the S_1 minimum to the S_1/S_0 minimum energy crossing points at ADC(2)/SV(P) level. The linearly interpolated coordinates (LIIC) are shown in Figure 3 (see also SI-5).

These energy profiles immediately answer the second question: C2 and C6 puckerings have significantly smaller energy barriers (about 0.38 eV) than EDPT (1.24 eV) for the *syn* conformer. Therefore, we expect puckering to be primarily favored. Constrained optimization of the EDPT barrier (open red points in Figure 3b) reduces it by a mere 0.2 eV, still favoring ring puckering mechanisms.

The computed S_0/S_1 density difference along the energy profiles shown in Figure 3 sheds light on the energy barrier's origin. (Density differences over the entire energy profiles are shown in SI-5.) The S_0/S_1 density differences for C2- and C6-puckerings are concentrated in the adenine moiety along the whole path (Figure 3a and SI-5 Figure S18 and S20). This means that the electron density from the S_1 minimum (an $n\pi^*$ state) to the state intersection does not drastically change along the reaction pathway. On the other hand, in the EDPT coordinate, the electronic density needs to be strongly rearranged over the whole molecule to cross the barrier (Figure 3b). At first, the density is concentrated on the adenine moiety at the S_1 minimum. Along the path, the hydrogen transfer is accompanied by a strong charge transfer from the lone pair of 5'-OH of the sugar, the negative region (green), to the π^* orbital of the adenine moiety, the positive region (orange).

To answer the third question, note that most trajectories of *syn*-adenosine quickly relax toward the S_1 minimum. From there, they deactivate via ring puckering due to its lower barriers. However, it takes some time, as climbing these barriers requires relatively large ring distortions, 2.1 $amu^{1/2}$Å (Figure 3a) for C2 and 3.6 $amu^{1/2}$Å for C6 (Figure S15-b). On the other hand, a few trajectories, reach the EDPT barrier, near the Franck Condon region (1.1 $amu^{1/2}$Å; Figure 3b), before relaxing to the S_1 minimum. Their subsequent proton transfer quickly induces internal conversion. Thus, the EDPT trajectories are fast but rare.

The energy barriers for C2-puckering are identical for *anti* and *syn* conformers (0.39 and 0.38 eV, respectively). They are also similar for C6-puckering, 0.36 eV for *syn,* and 0.32 eV for *anti*. However, the excited-state lifetime of the *anti* conformer (3.5 ps; Table 1) is much longer than that of the *syn* conformer (2.1 ps). Therefore, the intramolecular hydrogen bond's presence accelerates the dynamics somehow. As we can see comparing Figure 3a and c, the molecular distortions needed to reach the C2-puckered intersection are much smaller for *syn* than for *anti*. The mean mass-weighted distortion between the S_1/S_0 crossing point and the initial geometry considering all trajectories doing C2 puckering is 5 $amu^{1/2}$Å for *syn* and 12 $amu^{1/2}$Å for *anti* (SI Table S5). Among those doing C6 puckering, the mean distortion is 8 $amu^{1/2}$Å for *syn* and 11 $amu^{1/2}$Å for *anti*. The smaller distortions in *syn* are due to hydrogen-bond constraint, which prevents the sugar's rotation around the covalent bond, attaching it to adenine.

To conclude, we investigated the gas-phase nonadiabatic dynamics of two adenosine conformers with and without a hydrogen bond. Our findings show that hydrogen bond significantly speeds up the dynamics of the *syn* conformer. Nevertheless, the dynamics is dominated by ring puckering. EDPT, the alternative intramolecular hydrogen-transfer mechanism, was operative only for 20% of the trajectories. Moreover, adenosine dynamics should be slower than that of adenine. Previous experimental results claiming the opposite seem to have underestimated the time constant by not

considering the ionization potential dependence on the excited-state pathways. The main effect of the hydrogen bond in *syn*-adenosine's dynamics is to speed up the internal conversion through puckering by imposing restrictions on the sugar-adenine relative orientation.

Computational Methods

A comprehensive description of the computational methodology is delivered in the SI-6 and SI-7. In brief, nonadiabatic molecular dynamics were simulated using decoherence-corrected[27] fewest-switches surface hopping[28] (DC-FSSH), using the local diabatization algorithm,[29, 30] as implemented in Newton-X v2.2-B15 program.[31] Initial conditions were generated with a correlated quantum harmonic oscillator distribution. Four trajectory sets were run to test the conformer, the initial excitation energy, and the basis set effects. Their parameters are summarized in Table 2. Trajectories were propagated for up to 2 ps. Only hoppings between excited states were computed. Trajectories reaching an S_1/S_0 energy gap smaller than 0.15 eV were ended, and the corresponding time step was taken as a proxy for the excited-state deactivation time.

Table 2. Characterization of the four sets of trajectories. Initial conditions were selected within a narrow (±0.1 eV) energy window either at the lower region (LB) or the center (CB) of the first absorption band. For each geometry sampled, the bright state may have an adiabatic position within the energy window between S_1 and S_3. Thus in Set 3, for example, 12 trajectories started in S_2 and 18 in S_3. cc-pVDZ+ stands for aug-cc-pVDZ in N3 and cc-pVDZ in all other atoms.

Set	Conformer	Excitation (eV)	Level	# trajectories	Initial states
1	*anti*	LB: 5.1±0.1	ADC(2)/SV(P)	50	50 S_2
2	*syn*	LB: 5.1±0.1	ADC(2)/SV(P)	50	18 S_1 ; 24 S_2 ; 8 S_3
3	*syn*	CB: 5.3±0.1	ADC(2)/SV(P)	30	12 S_2; 18 S_3
4	*syn*	CB: 5.1±0.1	ADC(2)/cc-pVDZ+	30	6 S_1; 12 S_2; 12 S_3

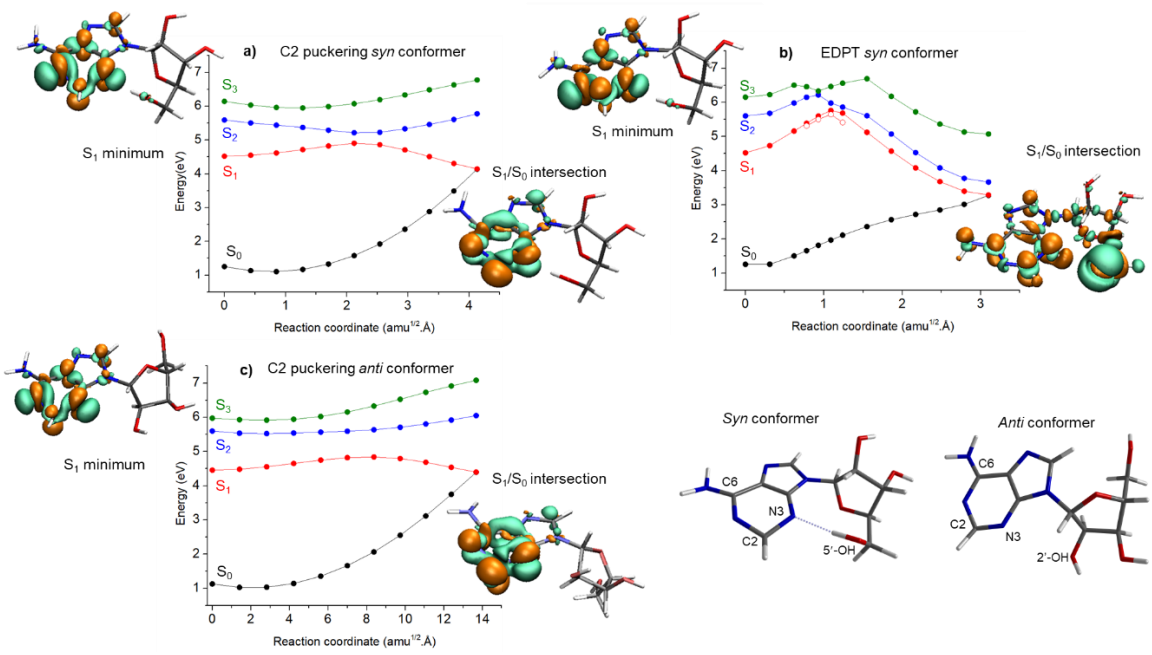

Figure 3. Energy profiles between the S_1 minimum and **(a)** C2-puckering intersection (*syn);* **(b)** EDPT intersection (*syn*); **(c)** C2-puckering intersection (*anti*). All LIIC calculations were done with ADC(2)/SV(P). Open circles on **(b)** denote optimized geometries imposing constraints to the 5´-OH---N3 and 5´-O---H bond lengths. Electron density difference maps (iso-value 0.005) along the proton transfer LIIC for *syn* and *anti* conformers at their S_1 minimum and S_1/S_0 intersection are shown as inserts. Negative regions (electron density decreasing) are shown in green and positive regions (electron density increasing) in orange.

The electronic structure method used in the dynamics and reaction pathways was the resolution-of the-identity algebraic diagrammatic construction to second-order [RI-ADC(2)][32-36] as implemented in Turbomole 7.3.[37] Trajectories sets 1 to 3 employed the SV(P) basis set. In Set 4, diffuse functions were added to N3 to test their effect on the EDPT pathway. The MP2 method was used for obtaining ground-state equilibrium geometries. For the S_1/S_0 crossing points, we used the CIOpt program.[38] Linearly interpolated pathways were computed between the S_1 minimum and the puckered intersections for both conformers. For *syn*, it was also computed between the S_1 minimum and the EDPT intersection.

ASSOCIATED CONTENT

Supporting Information

The Supporting information (PDF) is available free of charge. Supporting information contains excited-state characterization; details of the dynamics results; characterization of the state minima and intersections; ionization potentials; linear interpolations; simulated spectra and initial conditions; nonadiabatic dynamics setup.

AUTHOR INFORMATION

Corresponding Authors

*E-mail: josene-maria.toldo@univ-amu.fr

*E-mail: mario.barbatti@univ-amu.fr; website: www.barbatti.org

Data availability

The raw data is available for download at: https://doi.org/10.6084/m9.figshare.19794130.v1

AUTHOR INFORMATION

Notes

There are no conflicts to declare.

ACKNOWLEDGMENT

R. M. and M. B. thank the European Research Council (ERC) Advanced grant SubNano (Grant agreement 832237). J. M. T. and M. B. thank funding from the European Union's Horizon 2020 Research and Innovation programme under grant agreement 828753 (Boostcrop). The Centre de Calcul Intensif d'Aix-Marseille is acknowledged for granting access to its high-performance computing resources. This work was performed using HPC/AI resources from GENCI-TGCC (Grant 2022- A0110813035).

REFERENCES

(1) Crespo-Hernández, C. E.; Cohen, B.; Hare, P. M.; Kohler, B. Ultrafast Excited-State Dynamics in Nucleic Acids. *Chem. Rev.* **2004**, *104* (4), 1977-2020.

(2) Hare Patrick, M.; Crespo-Hernández Carlos, E.; Kohler, B. Internal conversion to the electronic ground state occurs via two distinct pathways for pyrimidine bases in aqueous solution. *Proc. Natl. Acad. Sci. U. S. A.* **2007**, *104* (2), 435-440.

(3) Borrego-Varillas, R.; Nenov, A.; Kabaciński, P.; Conti, I.; Ganzer, L.; Oriana, A.; Jaiswal, V. K.; Delfino, I.; Weingart, O.; Manzoni, C.; et al. Tracking excited state decay mechanisms of pyrimidine nucleosides in real time. *Nat. Commun.* **2021**, *12* (1), 7285.

(4) Pecourt, J.-M. L.; Peon, J.; Kohler, B. Ultrafast Internal Conversion of Electronically Excited RNA and DNA Nucleosides in Water. *J. Am. Chem. Soc.* **2000**, *122* (38), 9348-9349.

(5) Pecourt, J.-M. L.; Peon, J.; Kohler, B. DNA Excited-State Dynamics: Ultrafast Internal Conversion and Vibrational Cooling in a Series of Nucleosides. *J. Am. Chem. Soc.* **2001**, *123* (42), 10370-10378.

(6) Kohler, B. Nonradiative Decay Mechanisms in DNA Model Systems. *J. Phys. Chem. Lett.* **2010**, *1*, 2047-2053.

(7) Conti, I.; Garavelli, M. Evolution of the Excitonic State of DNA Stacked Thymines: Intrabase $\pi\pi^* \rightarrow$ S0 Decay Paths Account for Ultrafast (Subpicosecond) and Longer (>100 ps) Deactivations. *J. Phys. Chem. Lett.* **2018**, *9* (9), 2373-2379.

(8) Middleton, C. T.; de La Harpe, K.; Su, C.; Law, Y. K.; Crespo-Hernández, C. E.; Kohler, B. DNA Excited-State Dynamics: From Single Bases to the Double Helix. *Annu. Rev. Phys. Chem.* **2009**, *60* (1), 217-239.

(9) Ortín-Fernández, J.; González-Vázquez, J.; Martínez-Fernández, L.; Corral, I. Molecular Identification of the Transient Species Mediating the Deactivation Dynamics of Solvated Guanosine and Deazaguanosine. *Molecules* **2022**, *27* (3), 989.

(10) Barbatti, M.; Aquino, A. J. A.; Lischka, H. The UV absorption of nucleobases: semi-classical ab initio spectra simulations. *Phys. Chem. Chem. Phys.* **2010**, *12* (19), 4959-4967, 10.1039/B924956G.

(11) Plasser, F.; Crespo-Otero, R.; Pederzoli, M.; Pittner, J.; Lischka, H.; Barbatti, M. Surface Hopping Dynamics with Correlated Single-Reference Methods: 9H-Adenine as a Case Study. *J. Chem. Theory Comput.* **2014**, *10* (4), 1395-1405.

(12) Beckstead, A. A.; Zhang, Y.; de Vries, M. S.; Kohler, B. Life in the light: nucleic acid photoproperties as a legacy of chemical evolution. *Phys. Chem. Chem. Phys.* **2016**, *18* (35), 24228-24238.

(13) Plasser, F.; Aquino, A. J.; Lischka, H.; Nachtigallova, D. Electronic excitation processes in single-strand and double-strand DNA: a computational approach. *Top. Curr. Chem.* **2015**, *356*, 1-37.

(14) Barbatti, M.; Aquino, A. J. A.; Szymczak, J. J.; Nachtigallová, D.; Hobza, P.; Lischka, H. Relaxation mechanisms of UV-photoexcited DNA and RNA nucleobases. *Proc. Natl. Acad. Sci. U. S. A.* **2010**, *107* (50), 21453-21458.

(15) Barbatti, M.; Borin, A. C.; Ullrich, S. Photoinduced Processes in Nucleic Acids. *Top. Curr. Chem.* **2014**, *vol 355*, 1-32.

(16) Tuna, D.; Sobolewski, A. L.; Domcke, W. Mechanisms of Ultrafast Excited-State Deactivation in Adenosine. *J. Phys. Chem. A* **2014**, *118* (1), 122-127.

(17) Zhao, L.; Zhou, G.; Jia, B.; Teng, G.; Zhan, K.; Zheng, H.; Luo, J.; Liu, B. New insight into the ultrafast excited state deactivation mechanism of guanosine in the gas phase. *J. Photochem. Photobiol. A* **2020**, *401*, 112753.

(18) Asami, H.; Yagi, K.; Ohba, M.; Urashima, S.-H.; Saigusa, H. Stacked base-pair structures of adenine nucleosides stabilized by the formation of hydrogen-bonding network involving the two sugar groups. *Chem. Phys.* **2013**, *419*, 84-89.

(19) Camillis, S. D.; Miles, J.; Alexander, G.; Ghafur, O.; Williams, I. D.; Townsend, D.; Greenwood, J. B. Ultrafast non-radiative decay of gas-phase nucleosides. *Phys. Chem. Chem. Phys.* **2015**, *17* (36), 23643-23650.

(20) Canuel, C.; Mons, M.; Piuzzi, F.; Tardivel, B.; Dimicoli, I.; Elhanine, M. Excited states dynamics of DNA and RNA bases: Characterization of a stepwise deactivation pathway in the gas phase. *J. Chem. Phys.* **2005**, *122* (7), 074316.

(21) Nir, E.; Plützer, C.; Kleinermanns, K.; de Vries, M. Properties of isolated DNA bases, base pairs and nucleosides examined by laser spectroscopy. *Eur. Phys. J. D* **2002**, *20*, 317-329.

(22) Pepino, A. J.; Segarra-Marti, J.; Nenov, A.; Improta, R.; Garavelli, M. Resolving Ultrafast Photoinduced Deactivations in Water-Solvated Pyrimidine Nucleosides. *J. Phys. Chem. Lett.* **2017**, *8* (8), 1777-1783.

(23) Pepino, A. J.; Segarra-Marti, J.; Nenov, A.; Rivalta, I.; Improta, R.; Garavelli, M. UV-induced long-lived decays in solvated pyrimidine nucleosides resolved at the MS-CASPT2/MM level. *Phys. Chem. Chem. Phys.* **2018**, *20* (10), 6877-6890.

(24) Ivanov, A. Y.; Rubin, Y. V.; Egupov, S. A.; Belous, L. F.; Karachevtsev, V. A. The conformational structure of adenosine molecules, isolated in low-temperature Ar matrices. *Low Temp. Phys.* **2015**, *41* (11), 936-941.

(25) Canuel, C.; Mons, M.; Piuzzi, F.; Tardivel, B.; Dimicoli, I.; Elhanine, M. Excited states dynamics of DNA and RNA bases: characterization of a stepwise deactivation pathway in the gas phase. *J. Chem. Phys.* **2005**, *122* (7), 074316.

(26) Barbatti, M.; Ullrich, S. Ionization potentials of adenine along the internal conversion pathways. *Phys. Chem. Chem. Phys.* **2011**, *13* (34), 15492-15500.

(27) Granucci, G.; Persico, M. Critical appraisal of the fewest switches algorithm for surface hopping. *The Journal of Chemical Physics* **2007**, *126* (13), 134114.

(28) Tully, J. C. Molecular dynamics with electronic transitions. *J. Chem. Phys.* **1990**, *93*, 1061-1071.

(29) Granucci, G.; Persico, M.; Toniolo, A. Direct semiclassical simulation of photochemical processes with semiempirical wave functions. *The Journal of Chemical Physics* **2001**, *114*, 10608-10615.

(30) Plasser, F.; Granucci, G.; Pittner, J.; Barbatti, M.; Persico, M.; Lischka, H. Surface hopping dynamics using a locally diabatic formalism: charge transfer in the ethylene

dimer cation and excited state dynamics in the 2-pyridone dimer. *J. Chem. Phys.* **2012**, *137* (22), 22A514.

(31) Barbatti, M.; Ruckenbauer, M.; Plasser, F.; Pittner, J.; Granucci, G.; Persico, M.; Lischka, H. Newton-X: a surface-hopping program for nonadiabatic molecular dynamics. *WIREs: Comp. Mol. Sci.* **2013**, *4* (1), 26-33.

(32) Dreuw, A.; Wormit, M. The algebraic diagrammatic construction scheme for the polarization propagator for the calculation of excited states. *WIREs: Comp. Mol. Sci.* **2015**, *5* (1), 82-95.

(33) Schirmer, J. Beyond the random-phase approximation: A new approximation scheme for the polarization propagator. *Phys. Rev. A* **1982**, *26* (5), 2395-2416.

(34) Trofimov, A. B.; Schirmer, J. An efficient polarization propagator approach to valence electron excitation spectra. *J. Phys. B: At., Mol. Opt. Phys.* **1995**, *28* (12), 2299-2324.

(35) Hättig, C. Structure Optimizations for Excited States with Correlated Second-Order Methods: CC2 and ADC(2). In *Adv. Quantum Chem.*, Jensen, H. J. Å. Ed.; Vol. 50; Academic Press, 2005; pp 37-60.

(36) Hättig, C.; Hellweg, A.; Köhn, A. Distributed memory parallel implementation of energies and gradients for second-order Møller–Plesset perturbation theory with the resolution-of-the-identity approximation. *Phys. Chem. Chem. Phys.* **2006**, *8* (10), 1159-1169.

(37) Balasubramani, S. G.; Chen, G. P.; Coriani, S.; Diedenhofen, M.; Frank, M. S.; Franzke, Y. J.; Furche, F.; Grotjahn, R.; Harding, M. E.; Hättig, C.; et al. TURBOMOLE: Modular program suite for ab initio quantum-chemical and condensed-matter simulations. *The Journal of Chemical Physics* **2020**, *152* (18), 184107.

(38) Levine, B. G.; Coe, J. D.; Martínez, T. J. Optimizing Conical Intersections without Derivative Coupling Vectors: Application to Multistate Multireference Second-Order Perturbation Theory (MS-CASPT2). *J. Phys. Chem. B* **2008**, *112* (2), 405-413.